Conf-931133--7

LBL-34587
UC-404

Lawrence Berkeley Laboratory

UNIVERSITY OF CALIFORNIA

Materials Sciences Division

Presented at the Thirty-Eighth Conference on Magnetism and Materials, Minneapolis, MN, November 15–18, 1993, and to be published in the Proceedings

Giant Magnetoresistance and Microstructural Characteristics of Epitaxial Fe-Ag and Co-Ag Granular Thin Films

N. Thangaraj, C. Echer, K.M. Krishnan, R.F.C. Farrow, R.F. Marks, and S.S.P. Parkin

October 1993

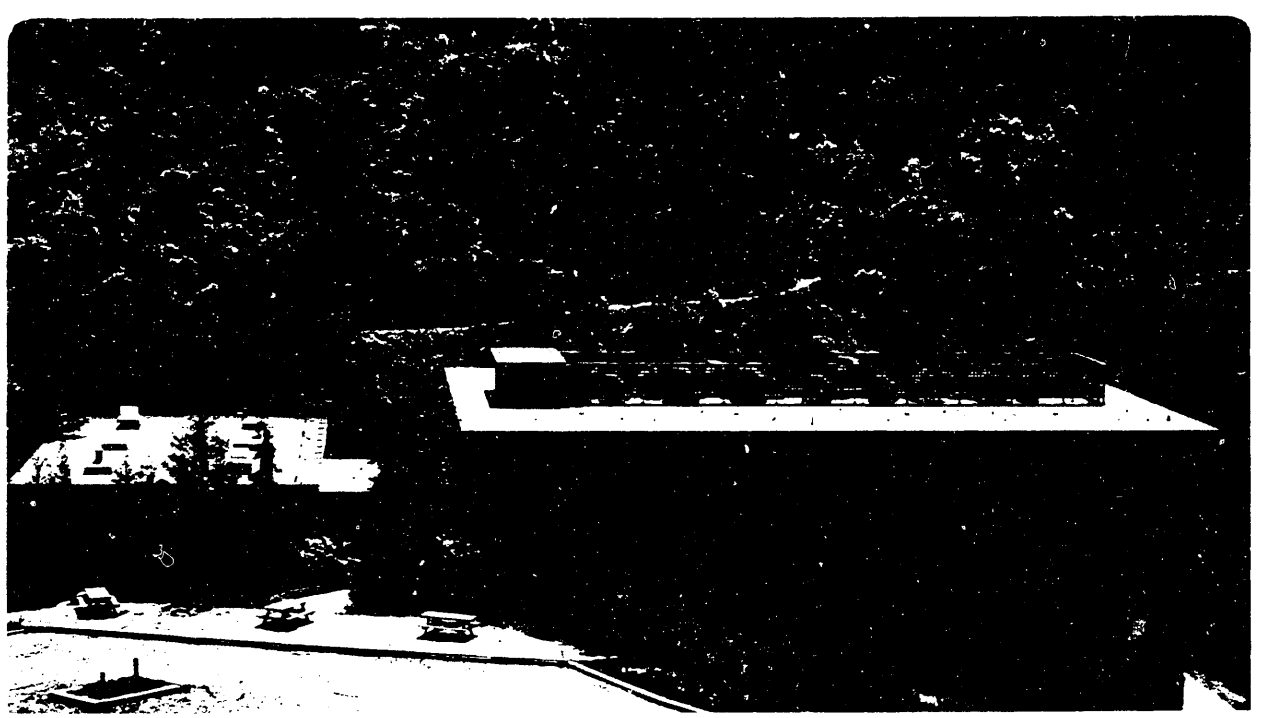

Prepared for the U.S. Department of Energy under Contract Number DE-AC03-76SF00098

LBL-34587

Giant Magnetoresistance and Microstructural Characteristics of Epitaxial Fe-Ag and Co-Ag Granular Thin Films

N. Thangaraj, C. Echer, K.M. Krishnan, R.F.C. Farrow*,
R.F. Marks*, and S.S.P. Parkin*

Materials Science Division
National Center for Electron Microscopy
Lawrence Berkeley Laboratory
University of California, Berkeley, CA 94720

*IBM Almaden Research Center
650 Harry Road
San Jose, CA. 95120

38th Conference on Magnetism & Magnetic Materials
November 15-18, 1993, Minneapolis, MN.

This work was supported in part by the Director, Office of Energy Research, Office of Basic Energy Sciences, Materials Science Division of the U.S. Department of Energy under Contract No. DE-AC03-76SF00098.

GIANT MAGNETORESISTANCE AND MICROSTRUCTURAL CHARACTERISTICS OF EPITAXIAL Fe-Ag AND Co-Ag GRANULAR THIN FILMS

N. Thangaraj, C. Echer and Kannan M. Krishnan

Materials Sciences Division, Lawrence Berkeley Laboratory, University of California, Berkeley, CA 94720

R. F. C. Farrow, R. F. Marks and S. S. P. Parkin

IBM Almaden Research Center, 650 Harry Road, San Jose, CA 95120

Abstract

The microstructure and magnetic properties of phase-separated Fe-Ag and Co-Ag granular alloy films, grown epitaxially on NaCl (001) substrates and exhibiting giant magnetoresistance (GMR) have been investigated. Surprisingly, two Fe-Ag films of similar composition grown under identical conditions are found to have substantially different microstructures yet display similar GMR. The microstructure of these films is characterized by Fe-rich or Co-rich regions respectively, 350-700 nm in extent, surrounded by a Ag-rich matrix. Within the Ag-rich regions, the Fe concentration varies from 20 to 25 atomic % and the Co concentration is ≅16 atomic %. Within these regions essentially pure fcc Co particles and bcc Fe particles are in parallel and rotated epitaxial alignment respectively with the fcc silver matrix. The Co and Fe particles are ≅15 to 25Å in diameter. It is these small particles which most likely account for the giant magnetoresistance exhibited by these alloys. This suggests that a size distribution of magnetic particles, sharply peaked at the optimum size with limited bulk segregation might give rise to larger GMR values.

PACS numbers: 72.15.-v, 64.80.Gd, 68.55.Nq

I. Introduction

Enhanced magnetoresistance, or giant magnetoresistance (GMR), is exhibited by a variety of different inhomogeneous metallic magnetic systems. The common feature of these systems is the presence of magnetic layers or particles separated by non-ferromagnetic material. In magnetic multilayers the largest GMR has been found in systems comprised of thin ≅ 8Å thick Co layers separated by thin (≅8Å) Cu layers.[1,2] In magnetic granular alloys the largest GMR has been reported in Co_xAg_{1-x} ($x \cong 0.2$).[3-5] A variety of models have been proposed to account for the origin of the GMR effect.[6-8] Of particular interest is the relationship of GMR to the detailed microstructure of the magnetic multilayer or alloy. The basic assumption of most models of GMR is the existence of spin-dependent scattering of the conduction electron either within the interior (bulk) of the magnetic layers or particles or at the interfaces between the magnetic and non-magnetic entities. Recent experiments strongly suggest the predominant role of interfacial scattering in accounting for the GMR of both multilayers[9-11] and granular alloys.[3,5,12] For the latter this means that the size of the magnetic particles is a key parameter in determining the magnitude of GMR.

Typically magnetic granular films deposited by sputtering techniques at room temperature display little GMR. However GMR is obtained with appropriate post-growth annealing. In contrast, it has been shown recently that slow co-evaporation using electron beam or thermal evaporation sources under UHV conditions at moderate substrate temperatures of 250°C (less than required for post-growth annealing of sputtered films i.e. ≅400°C) yields GMR in the as-grown films in Co-Ag, Co-Cu and Fe-Ag.[5,12,13] In this paper, we report observations of the microstructure,

including features such as defects, magnetic particle size, distribution and composition, of Fe-Ag and Co-Ag thin films grown epitaxially on NaCl (001) substrates from transmission electron microscopy (TEM) studies.

II. Experimental Procedure

Fe-Ag and Co-Ag films were grown by slow co-evaporation of Fe or Co respectively, and Ag in a molecular beam epitaxy (MBE) system. The nominal compositions of Fe-Ag and Co-Ag thin films were ≅29 at% Fe and ≅21 at% Co, respectively. The NaCl substrates were cleaved in air and cleaned *in situ* at 300°C in ultra-high-vacuum (UHV) before growth. Thin films (≅500Å thick) highly oriented in the (001) direction were then grown at a substrate temperature of 250°C. No post-growth annealing was required to observe the GMR effect. Details of the growth and the magnetoresistance measurements of these and similar films grown on sapphire (0001) substrates are reported elsewhere.[5] For TEM studies, the films were lifted onto Cu grids by dissolving the NaCl substrate in water and the Pt cap layer was then removed by gentle ion-milling. Energy-dispersive x-ray microanalysis, and standard bright-field and dark-field TEM imaging techniques were used to analyze the microstructure of the films.

III. Microstructural Characteristics of Fe-Ag and Co-Ag Granular Alloy Films

A typical low magnification thorough-foil bright field TEM image of a $Fe_{29}Ag_{71}$ film is shown in figure 1a. Also included in the inset to the figure is the corresponding diffraction pattern which demonstrates the epitaxial growth of the film. The film microstructure is clearly inhomogeneous. The micrograph shows a distribution of

dark (pure Ag, 350-500 nm), gray (25 at% Fe, matrix) and light (88 at% Fe, 350-700 nm) regions. The microstructure also varies locally, indicating variations in metal film nucleation on the NaCl surface. Where the NaCl surface has a large local density of (001) steps, the microstructure contains about equal amount of Ag-rich (gray) and Fe-rich (light) regions. In addition, growth twins (≅30 nm size) form on the (111) planes of Ag. Four twin variants, typical of epitaxial fcc growth on NaCl (001) substrates are observed. From the electron diffraction pattern, the orientation relationship is clearly (100) Fe ‖ (100) Ag and $[01\bar{1}]$ Fe ‖ $[00\bar{1}]$ Ag, i.e. the reflections from the bcc Fe and the fcc Ag are in exact coincidence but rotated 45°(the lattices have only 0.8% mismatch in this arrangement). The presence of the fcc (γ) phase of Fe in the post-annealed Fe-Ag sample, as reported by Tsoukatos *et al*[14], has not been identified in our Fe-Ag samples. Another $Fe_{25}Ag_{75}$ deposition on NaCl under similar conditions unexpectedly resulted in a fine-grained polycrystalline film with slight (001) texture (figure 1(b)). For this film the particle size distribution is highly uniform with Fe concentration varying locally from 10-20 at%. However, a few isolated grains have a higher (30 at%) Fe concentration. For both samples, dark field imaging obtained from (200) Ag did not yield any information about the distribution and size of the phase-separated Fe particles because of the overlapping of Fe and Ag reflections.

The microstructure of the $Co_{21}Ag_{79}$ films (figure 2(a)) is similar to the epitaxial $Fe_{29}Ag_{71}$ microstructure (figure 1(a)). The microstructure consists of about 10% "Co-rich" light regions where the concentration varies from 32 to 64 at% Co (in most of the regions the Co concentration is above 50%). In contrast, the gray regions contain about 16 at% Co and these regions dominate the microstructure. However, where the Co-Ag film nucleates near steps on the

(001) NaCl, the volume fraction of Co-rich light regions increases and reaches about 50% (figure 2(b)). The (001) electron diffraction pattern obtained from the same area (fig. 2a, inset) confirms epitaxial growth of the Co-Ag films on NaCl (001). This pattern also shows distinct spots corresponding to phase separated fcc Co. Even though the Co_{fcc} and Ag_{fcc} have 13% lattice mismatch in the cube-cube orientation, the Co grows in epitaxial alignment with the Ag presumably due to high adatom mobility in this growth mode. Co particles within the Ag matrix retain their bulk lattice parameter and thus the 13% strain between the Co and the Ag lattices must be mostly accommodated at the interfaces. Dark-field imaging using the (220) Co reflection clearly shows the Co particle distribution and size (figure 2(c)). The Co particle size varies from 15 to 25Å, the mean "diameter" being 20Å. The inter-particle distance (figure 2(c)) appears similar to the particle size. However, this is not conclusive since the particles contained in the 500Å thick film are in projection in this TEM image. This measurement agrees with earlier studies[5] using grazing incidence small angle x-ray scattering (GISAXS) for a Co-Ag film grown on sapphire (0001) which showed comparable mean Co particle size (≅25Å) but a different mean inter-particle distance (≅76Å). As mentioned earlier, growth twins of Ag as well as Co are also present in this film. The Ag twins are about 700 to 1200Å in size. The Co twin size could not be established due to very weak diffraction.

IV. Magnetic Characterization of Fe-Ag and Co-Ag Granular Alloy Films

Although the microstructures of the two Fe-Ag films shown in figures 1(a) and (b) are quite different, the films exhibit similar MR as shown in figure 3. Both films show decreases in resistance (for applied fields of upto 16 KOe) of

about 4-5% at room temperature and 15% at 4.2 K. Similar values have also been reported for the post-annealed sputtered Fe-Ag samples.[14] An interesting feature of the data is that the GMR reveals distinct magnetic anisotropy for field applied perpendicular and parallel to the film as shown by the solid and dashed curves respectively in figure 3. A similar result has previously been found in MBE deposited Co-Ag alloy films for which various possible mechanisms were discussed.[5]

The magnetoresistance data for the Co-Ag film measured at room temperature is given in figure 4. A resistance change of 22% under a field of 60 KOe was observed. By varying Co composition, GMR of 40% at room temperature and 71% at 4.2 K has been observed for similar films grown on sapphire substrates.[5]

V. Discussions and Conclusions

If spin dependent electron scattering at the interfaces between the magnetic particles and the host non-ferromagnetic metal is the dominant scattering mechanism for GMR, then it follows that the magnitude of the GMR will scale approximately as the inverse particle size. Thus maximum GMR is expected for small magnetic particles. Annealing studies on MBE grown Co-Cu granular alloys show that the GMR is significantly reduced by annealing resulting from growth of the Co particles.[12] The TEM studies presented here show that a significant fraction, ≅50-90%, of the Co-Ag sample is comprised of small Co particles, ≅20Å in diameter, in a Ag matrix. These results are consistent with our earlier x-ray studies of the size and distribution of the Co particles in similarly prepared Co-Ag alloys.[5] Larger GMR is likely to be obtained by the preparation of alloys containing uniformly small Co particles.

Moreover any dissolution of the Co in the matrix is likely to lead to reduced GMR.[5]

A surprising result of these studies is the similarity of the GMR exhibited by the single crystalline and polycrystalline Fe-Ag alloys grown on NaCl substrates. The microstructure of these films is quite distinct. Moreover the GMR of these films is also similar to <111> oriented Fe-Ag films of the same composition grown on a Pt buffer layer on (0001) sapphire. This suggests that crystalline orientation is not a very significant factor in influencing the GMR or magnetic anisotropy of the Fe-Ag granular films. We note usually there is a much wider variation in GMR properties with different preparation and growth conditions. However for magnetic multilayers the magnitude of GMR is directly connected to the degree of antiferromagnetic alignment of the magnetic layers. This can be very sensitive to structural defects, especially for multilayers containing thin spacer layers. This means that GMR exhibited by multilayers is often more sensitive to structural defects than that found in granular alloys.

Acknowledgements

This research is supported by the Director, Office of Energy Research, Office of Basic Energy Sciences, Materials Sciences Division of the US Department of Energy under contract No. DE-AC03-76SF00098.

References

1. S. S. P. Parkin, R. Bhadra and K. P. Roche, Phys. Rev. Lett. **66**, 2152 (1991).

2. S. S. P. Parkin, Z. G. Li and D. J. Smith, Appl. Phys. Lett. **58**, 2710 (1991).

3. A. E. Berkowitz, J. R. Mitchell, M. J. Carey, A. P. Young, S. Zhang, F. E. Spada, F. T. Parker, A. Hutten and G. Thomas, Phys. Rev. Lett. **68**, 3745 (1992).

4. J. Q. Xiao, J. S. Jiang and C. L. Chien, Phys. Rev. Lett. **68**, 3749 (1992).

5. S. S. P. Parkin, R. F. C. Farrow, T. A. Rabedeau, R. F. Marks, G. R. Harp and Q. Lam, C. Chappert, M. F. Toney, R. Savoy and R. Geiss, Euro. Phys. Lett. **22**, 455 (1993).

6. R. E. Camley and J. Barnas, Phys. Rev. Lett. **63**, 664 (1989).

7. P. M. Levy, S. Zhang and A. Fert, Phys. Rev. Lett. **65**, 1643 (1990).

8. D. M. Edwards, R. B. Muniz and J. Mathon, IEEE Trans. Mag. **27**, 3548 (1991).

9. E. E. Fullerton, D. M. Kelly, J. Guimpel, I. K. Schuller and Y. Bruynseraede, Phys. Rev. Lett. **68**, 859 (1992).

10. S. S. P. Parkin, Appl. Phys. Lett. **61**, 1358 (1992).

11. S. S. P. Parkin, Phys. Rev. Lett. **71**, 1641 (1993).

12. T. A. Rabedeau, M. Toney, R. F. Marks, S. S. P. Parkin, R. F. C. Farrow and G. Harp, Phys. Rev. Lett. (submitted).

13. R. F. Marks, R. F. C. Farrow, G. R. Harp, S. S. P. Parkin, T. A. Rabedeau, M. F. Toney, A. Cebollada, N. Thangaraj, and K. M. Krishnan, (Mat. Res. Soc. Symp. Proc., 1993) Vol. 313.

14. A. Tsoukatos, H. Wan, G. C. Hadjipanayis and Z. G. Li, Appl. Phys. Lett. **61**, 3059 (1992).

15. S. S. P. Parkin, A. Modak and D. J. Smith, Phys. Rev. B **47**, 9136 (1993).

Figure Captions

Figure 1

(a) Microstructure of an as-deposited $Fe_{29}Ag_{71}$ on NaCl (001). The micrograph shows bulk segregation of Fe in the light region, pure silver particles in dark contrast, and the gray region with 25 at% Fe. The diffraction pattern shown in the inset indicates the (001) epitaxy of the film with the (001) NaCl substrate. (b) A second Fe-Ag film prepared under almost identical growth conditions shows a more uniform microstructure with a polycrystalline structure.

Figure 2

Microstructure of a $Co_{21}Ag_{79}$ sample showing (a) segregated Co-rich light regions grown on the flat NaCl surface and (b) regions of the film grown on the (001) NaCl steps. The inset in figure 1(a) is the electron diffraction pattern showing spot-splitting (arrow) due to Co-phase segregation and epitaxial alignment of Co particles with Ag. (c) Dark-field micrograph obtained using (220) Co reflection showing distribution of 20Å Co particles in the gray region.

Figure 3

(a) and (b) Magnetoresistance data at 295 K and at 4.2 K for the Fe-Ag film shown in figure 1(b). Figure (c) and (d) shows the magnetoresistance data for the Fe-Ag film shown in figure 1(a). The dashed lines are for the field aligned in the plane and the solid lines are for the field perpendicular to the film plane. The data show significant perpendicular magnetic anisotropy.

Figure 4

Magnetoresistance data measured at room temperature for the $Co_{21}Ag_{79}$ sample.

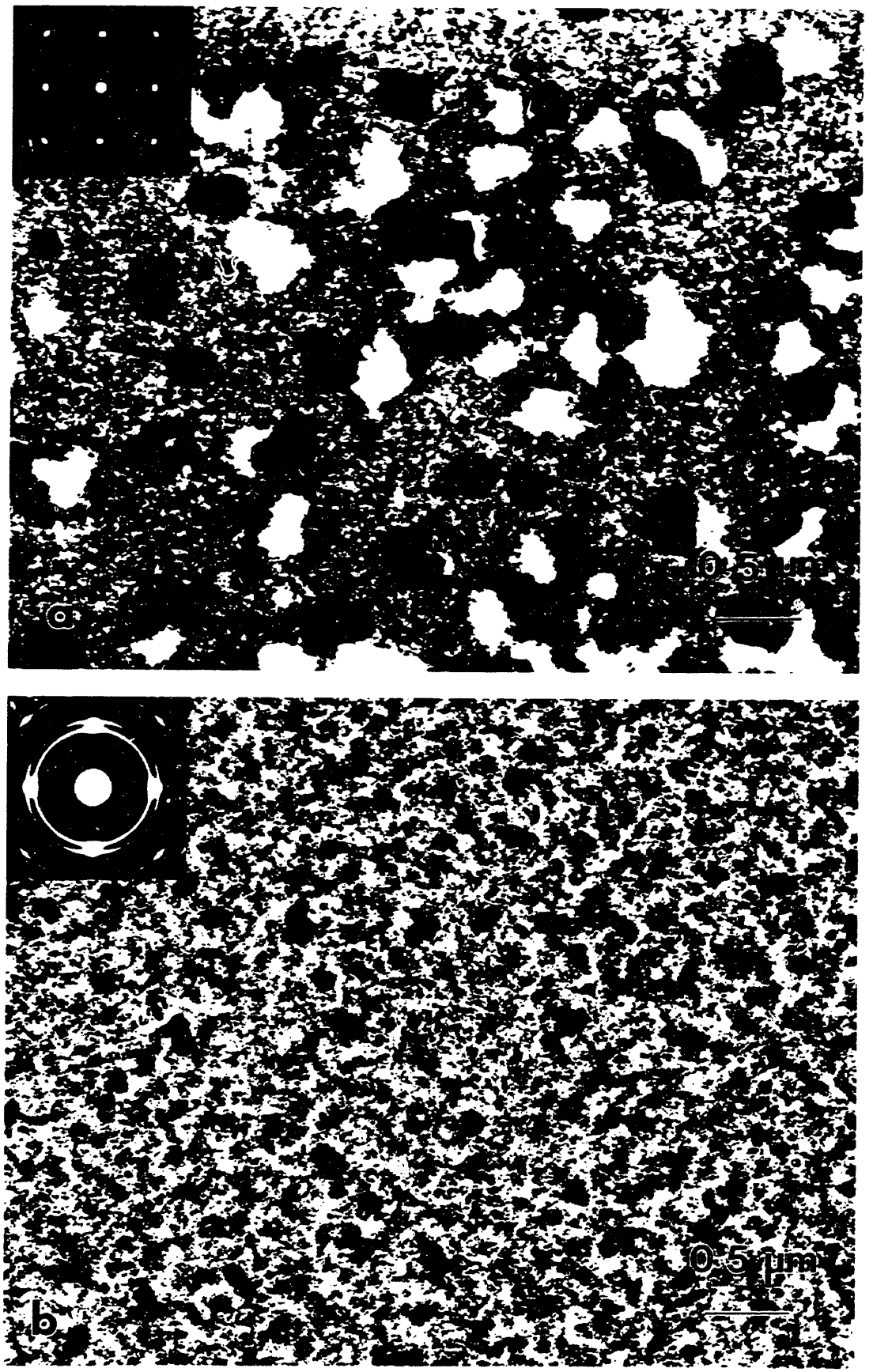

XBB 939-5778

Figure 1a & 1b

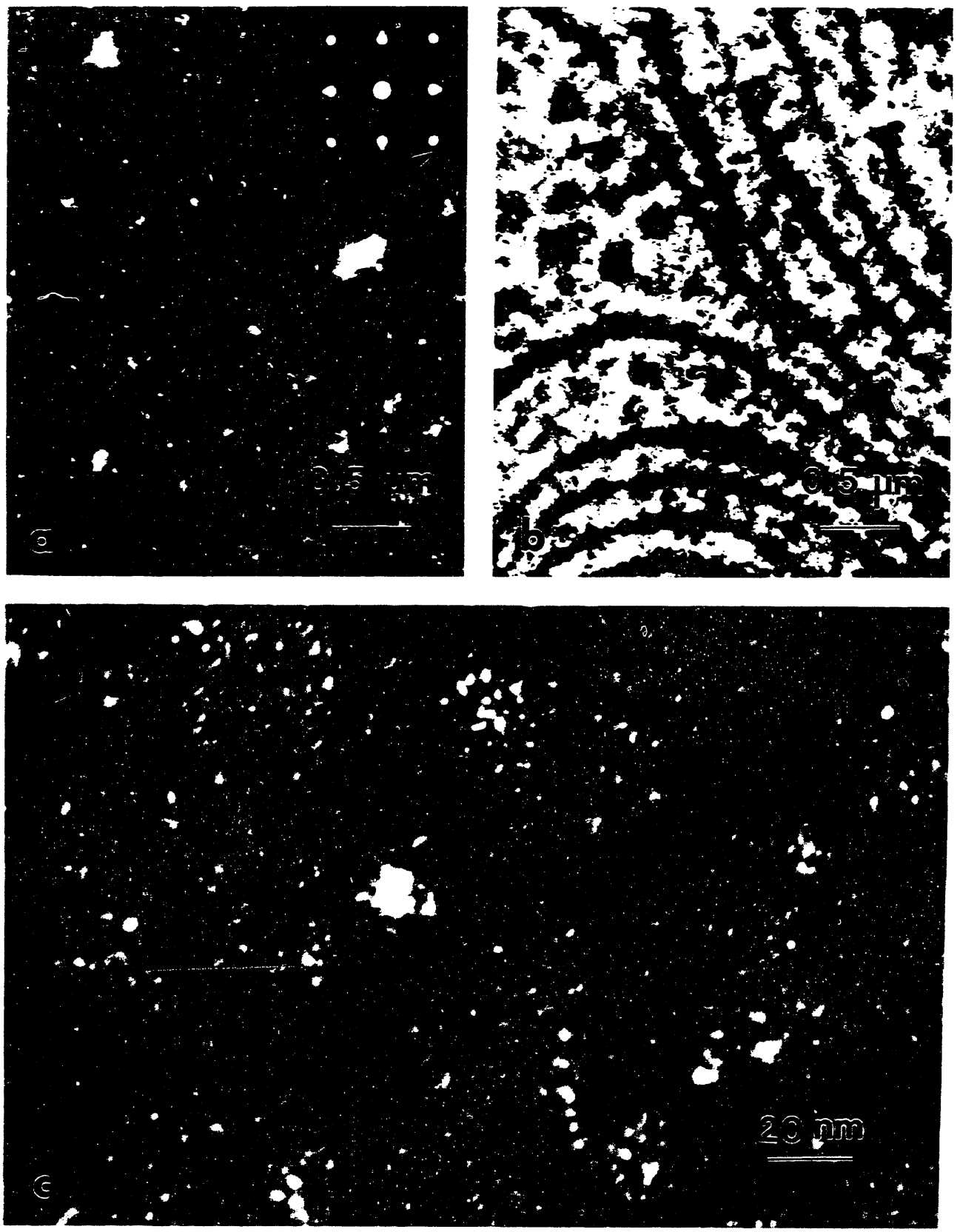

XBB 939-5779

Figure 2 a-c

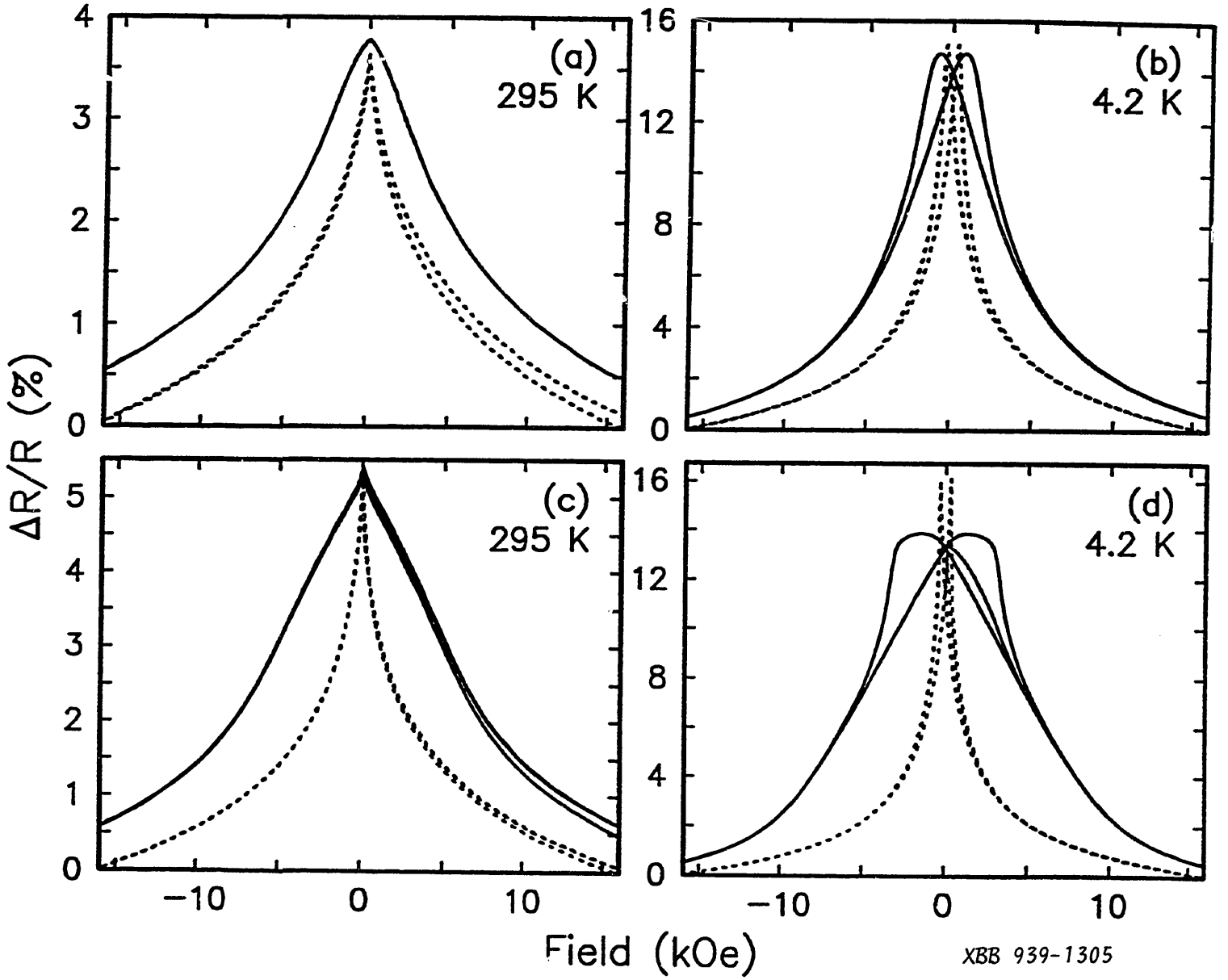

Figure 3

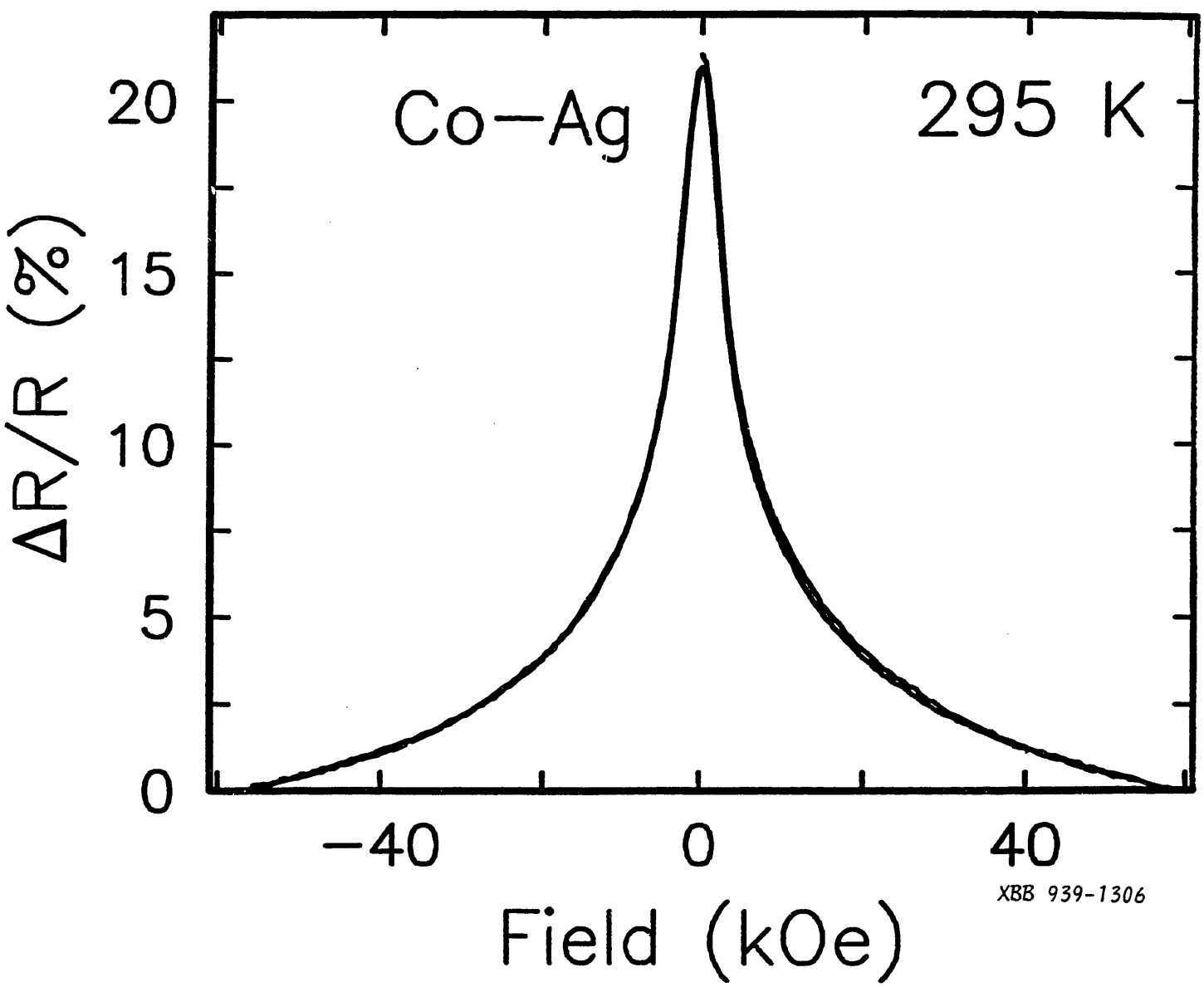

Figure 4

END

DATE
FILMED
3/9/94